Kullback-Leibler Distance Optimization for Non-rigid Registration of Echo-Planar to Structural Magnetic Resonance Brain Images

Ali Gholipour[1], Nasser Kehtarnavaz[1], Richard W. Briggs[2], Kaundinya S. Gopinath[2]

[1]Dept. of Electrical Engineering, University of Texas at Dallas, Richardson, TX,
[2]Dept. of Radiology, Neuroradiology Division, University of Texas Southwestern Medical Center, Dallas, TX,

ABSTRACT

This paper presents the use of Kullback-Leibler Distance (KLD) as part of an optimization framework to incorporate prior knowledge from field maps into non-rigid registration of echo-planar (EPI) to structural magnetic resonance brain images. An analytical expression is derived for the derivatives of KLD with respect to registration transformation parameters, which is shown to be computationally more efficient as compared to the derivatives of mutual information. Quantitative gold standard validation is carried out on simulated digital brain phantom images with synthesized deformations. In addition, in-vivo validation is performed via a cross-comparison of the similarity of high-resolution and low-resolution EPI to T1- and T2-weighted structural images. The results obtained indicate that the developed KLD-based non-rigid registration technique provides an effective way of correcting local distortions in echo-planar imaging.

Index Terms – Non-rigid Image Registration, Magnetic Resonance Echo-Planar Imaging, Kullback-Leibler Distance.

1. INTRODUCTION

Magnetic resonance Echo Planar Imaging (EPI) is widely used as a fast data acquisition technique providing acceptable time resolution for functional brain imaging. It is also deemed appropriate for the acquisition of large MR datasets on Diffusion Tensor Imaging (DTI) and Arterial Spin Labeling (ASL).However, EPI images suffer from spatial distortions that are mainly caused by magnetic field inhomogeneity artifacts. The accumulation of error over the long duration of phase encoding causes significant spatial distortions in the phase encoding direction of EPI images [1]. Such distortions can compromise the accuracy of functional activation detection and functional localization [2], as well as the analysis of DTI and ASL EPI datasets.

One approach to retrospective distortion correction in EPI is non-rigid registration to an undistorted structural MRI [3],[4],[5]. There has been considerable progress on inter-subject and subject-to-template non-rigid registration of high-resolution brain structural scans [2]. However, the application of non-rigid registration to EPI is much more challenging due to the characteristics of EPI images, which include unclear structural features, limited spatial resolution, and local nonlinear distortions. Finding local correspondences between EPI and high-resolution structural images is problematic. The few studies of non-rigid registration of EPI to structural MRI have relied on intensity-based similarity measures, specifically the Mutual Information (MI) measure [2]-[5]. In comparison to the physics-based constraints that are used in [3] and [4] for spin-echo and gradient-echo EPI images, hard parameter constraints are utilized in [5] within a limited memory bound constraint optimization algorithm (L-BFGS-B) [6], which was originally used in [7] for non-rigid registration of PET and CT images of the chest. More recently, in an MI-based technique, estimation of field map images are used as a guiding mechanism to constrain the transformation model to the distortion regions [8].

This paper presents an approach to improve the accuracy and reliability of the non-rigid registration technique discussed in [5] by utilizing the concept of the Kullback-Leibler Distance (KLD) measure in information theory [9]. This concept has been primarily used in rigid multi-modal registration of digital subtraction angiogram to magnetic resonance angiogram images [10]. Among the few recent studies that have utilized KLD as a similarity measure [10]-[13], only one [13] has addressed the non-rigid registration problem. Two main issues are addressed in this work. First, in most of the previous studies, pre-aligned images have been considered to serve as prior knowledge, while in practice such pre-alignments may not exist or may not be accurate for in-vivo images. Second, the computation of KLD and its derivatives is an important issue when considering high-dimensional non-rigid registration. The derivatives of this measure should be computed with respect to all the transformation parameters during each iteration, which is computationally quite inefficient if done with finite element methods. This issue has been discussed for MI in [7],[14] and for KLD using Gaussian function models in [13].

The idea of using KLD in this work is to incorporate prior knowledge from field maps into the non-rigid registration algorithm, not only by constraining the deformation field parameters (as discussed in [8]), but also in computing the similarity. An efficient general-purpose computation of KLD and its derivatives is formulated using B-Spline basis functions in section 2 and is subsequently modified for the functional imaging registration application. In section 3, the local performance of KLD and MI measures and quantitative gold standard validation are presented based on digital brain phantom images with simulated deformations. This section also includes an in-vivo validation via a cross-comparison of the similarity of high-resolution and low-resolution EPI with T1- and T2-weighted MR images.

2. NON-RIGID REGISTRATION

2.1. Optimization Framework

Mathematically, the source and target images can be modeled as two functions, $I_s : \Re^3 \to \Re$ and $I_t : \Re^3 \to \Re$, which associate scalar intensity values to points described by $\underline{x} = (x, y, z)$ in the three-dimensional vector space $\Re^3$. The target image, a high-resolution undistorted structural MR image, is fixed, and the source

image, the distorted echo-planar image, undergo a spatial vector transformation of the form

$$T(\underline{x}): \Re^3 \to \Re^3 \tag{1}$$

The registration problem is aimed at finding an appropriate transformation T to establish the most accurate mapping between the functional image space and the anatomical image space. The accuracy of such a mapping is defined based on the correspondences between the two images, and can be quantified by a cost function reflecting the dissimilarity of the transformed source and target images. That is

$$J(I_t, I_s \circ T) = J(T): \mathrm{T} \to \Re \tag{2}$$

where T is the set of admissible transformation functions. Then, an optimization procedure is performed to minimize this cost function

$$T_{opt} = \arg\min_{T \in \mathrm{T}} J(T) \tag{3}$$

where T_{opt} denotes the solution to the registration problem.

The choice of an optimization algorithm is critical in multi-modality non-rigid registration. The algorithm chosen here is L-BFGS-B, a quasi Newton optimization algorithm based on the so-called limited memory BFGS (Broyden, Fletcher, Goldfarb, and Shanno) matrices for estimation of the Hessian matrix [6]. One of the most important features of L-BFGS-B is its capacity for posing constraints on the parameters, which is discussed in section 2.2.

2.2. Transformation Model

The transformation model utilized here is a parametric free-form deformation model with a regular grid of control points. The deformation model is defined by three displacement parameters for each of the control points and the deformation at any point of the image is computed by a separable cubic B-Spline interpolation on the local control point displacements [5]. By choosing appropriate control point grid spacing, coarser than the image spacing, a trade-off between smoothness and local resolution of deformation is obtained. Due to the characteristics of B-Spline basis functions, this model is locally controllable, globally smooth and differentiable with respect to the deformation parameters. The latter is critical in computing the derivative of similarity measures (section 2.3).

As part of the L-BFGS-B optimization process, it is possible to use prior knowledge to pose constraints on the parameters of the described transformation model. For EPI, such prior knowledge can be obtained by physical analysis and field map acquisitions. Physical analysis shows that the effect of spatial distortions in EPI is much more significant in the phase encoding direction [1]; and phase images obtained from field map acquisitions can be used as a guide to detect distortion regions, i.e. for weighting the parameter bound constraints via estimating the magnitude of distortion.

2.3. Kullback-Leibler Distance and its Derivative

Kullback-Leibler Distance (KLD) is a measure of distance between two probability density functions (*pdf*s) [9] which are considered to be a reference and a test *pdf* here. KLD is minimal when the *pdf*s are equal. The idea of utilizing KLD in non-rigid registration of EPI to structural MRI is to incorporate prior knowledge into the registration framework. Field map acquisitions show that only parts of an EPI image, e.g. parts of the inferior frontal cortex near the air-tissue interfaces (sinuses) and the inferior temporal lobes, are affected by spatial distortions. Hence, it is possible to compute a reference joint *pdf* between EPI and structural images on the undistorted brain region. This reference joint *pdf* is simply an estimation of the joint histogram of the two images on the undistorted region, and is represented by $p^{\circ}(\nu, \kappa; \mu)$ as a function of transformation parameters (μ), where $0 \le \nu \le L_s$ and $0 \le \kappa \le L_t$ denote the indices of the histogram bins, and L_s and L_t are the numbers of bins over the intensity values of the source and target images. The test joint *pdf* is defined on the entire brain and is represented by $p(\nu, \kappa; \mu)$. KLD is then defined as

$$KLD(\mu) = \sum_{\nu} \sum_{\kappa} p(\nu, \kappa; \mu) \log \frac{p(\nu, \kappa; \mu)}{p^{\circ}(\nu, \kappa; \mu)} \tag{4}$$

The minimization of KLD results in those transformation parameters which maximize the similarity of the reference and test joint *pdf*s.

The derivative of KLD with respect to the transformation parameters is needed for optimization, and is given by

$$\frac{\partial KLD(\mu)}{\partial \mu} = \tag{5}$$

$$\sum_{\nu} \sum_{\kappa} \left(\left(1 + \log \frac{p(\nu, \kappa; \mu)}{p^{\circ}(\nu, \kappa; \mu)} \right) \frac{\partial p(\nu, \kappa; \mu)}{\partial \mu} - \left(\frac{p(\nu, \kappa; \mu)}{p^{\circ}(\nu, \kappa; \mu)} \right) \frac{\partial p^{\circ}(\nu, \kappa; \mu)}{\partial \mu} \right)$$

This derivative depends on the partial derivatives of the joint *pdf*s. To have an efficient computation of the derivatives of the joint *pdf*s, Parzen window models using separable B-Spline kernels can be used [7],[14]. For both the reference and test joint *pdf*s, a zero-order B-Spline kernel $\beta^{(0)}(.)$ is used for the target image, and a cubic B-Spline kernel $\beta^{(3)}(.)$ is used for the source image. Only the source image is transformed and this choice guarantees the smoothness of derivative computations. As a result, the smooth model of the joint histogram of $(I_t, I_s \circ T)$ can be written as

$$p(\nu, \kappa; \mu) = \frac{1}{card(V)} \sum_{x \in V} \beta^{(0)} \left(\kappa - \frac{I_t(\underline{x}) - I_t^{\circ}}{\Delta b_t} \right) \times \beta^{(3)} \left(\nu - \frac{I_s \circ T(\underline{x}; \mu) - I_s^{\circ}}{\Delta b_s} \right) \tag{6}$$

where *V* is a subset of voxels used in the computation of the joint *pdf*; and the voxel values for the images are normalized according to the minimum intensity values (I_t° and I_s°), and the intensity range of each histogram bin (Δb_t and Δb_s).

Note that the marginal *pdf* of the target image ($p_t(\kappa)$) is the sum of the zero-order B-Spline functions in the separable formulation of equation (6), and is independent of the transformation parameters (μ). Therefore, the very first term inside the summations of equation (5) is zero since

$$\sum_{\kappa \in L_t} \sum_{\nu \in L_s} \partial p(\nu, \kappa; \mu) / \partial \mu = \sum_{\kappa \in L_t} \partial p_t(\kappa) / \partial \mu = 0.$$

It is worth mentioning that KLD provides a general definition for MI. The definition of MI is derived from (4) by substituting $p^{\circ}(\nu, \kappa; \mu) = p_t(\kappa) p_s(\nu; \mu)$, where $p_s(\nu; \mu)$ is the marginal *pdf* of the source image. Simplification of (5) with this substitution gives an expression for the derivative of MI, which complies with the expression derived in [14]

$$\frac{\partial MI(\mu)}{\partial \mu} = \sum_{\nu} \sum_{\kappa} \left(\log \frac{p(\nu, \kappa; \mu)}{p_s(\nu; \mu)} \right) \frac{\partial p(\nu, \kappa; \mu)}{\partial \mu} \tag{7}$$

Going back to the derivatives of KLD measure in equation (4), further simplification of the registration algorithm is made possible by constraining the transformation parameters to the distortion regions. When the deformation is locally applied to the distortion regions, the reference joint *pdf* is not a function of μ, and this simple formula is obtained for the derivatives of KLD:

$$\frac{\partial KLD(\mu)}{\partial \mu} = \sum_{\nu}\sum_{\kappa}\left(\log\frac{p(\nu,\kappa;\mu)}{p^{\circ}(\nu,\kappa)}\right)\frac{\partial p(\nu,\kappa;\mu)}{\partial \mu} \quad (8)$$

The reference joint *pdf* is computed once at the beginning of the registration algorithm. Consequently, the iterative computation of KLD derivatives in equation (7) is computationally more efficient than MI in equation (8) (the marginal *pdf* of the source image is computed during each iteration). Furthermore, it incorporates the prior knowledge into the registration framework.

According to (7) and (8), only the derivative of the test joint *pdf* is needed for the optimization. The derivative of the joint *pdf* as estimated in equation (6) is found by applying the chain rule [7], that is

$$\frac{\partial p(\nu,\kappa;\mu)}{\partial \mu} = \frac{1}{card(V).\Delta b_s}\sum \beta^{(0)}\left(\kappa - \frac{I_t(\underline{x}) - I_t^{\circ}}{\Delta b_t}\right)\times \quad (9)$$

$$\left.\frac{\partial \beta^{(3)}(u)}{\partial u}\right|_{u=\nu-\left(I_s\circ T(\underline{x};\mu)-I_s^{*}\right)/\Delta b_s} \times \left(\left.\frac{-\partial I_s(\underline{y})}{\partial \underline{y}}\right|_{\underline{y}=T(\underline{x};\mu)}\right)^{T}\times\frac{\partial T(\underline{x};\mu)}{\partial \mu}$$

The second product term in (9) is explicitly computed as a subtraction of two second-order B-Spline kernels [15]. The third product term is the gradient of the source image on a transformed point, and can be computed by finite element methods or using the derivative of B-Spline functions when B-Spline interpolation is applied. Finally, since the transformation model described in section 2.2 ([5], [3], [7]) is linear with respect to the transformation parameters, the last term simply denotes the coefficients of each of the parameters in the appropriate direction. By using the L-BFGS-B optimization algorithm, the Hessian matrix is estimated through curvature using limited memory BFGS matrices [6] and thus there is no need for the computation of the second derivatives of (9).

3. EXPERIMENTS

3.1. Quantitative Gold Standard Validation

Quantitative validation was achieved in two steps using the *Brainweb* [16] digital brain phantom database. First local performance of KLD was considered in the presence of local synthetic deformations. Second, the registration algorithm was applied for the correction of synthetic deformations on simulated low-resolution PD-MRI images resembling the limitations of EPI. Figure 1 shows that KLD always reached a minimum level at the center of a local deformation synthesized on both high-resolution T2-weighted MRI and low-resolution (LR) PD-MRI. The reference joint *pdf* was computed on the undistorted regions between these images and the *Brainweb* high-resolution T1-weighted image; and the test joint *pdf* was computed on the entire brain (solid and dashed lines) and on the distortion region only (the dotted line). Figure 2 shows that for ten registration experiments that were done using the gold standard digital brain phantom simulated EPI and T1-weighted MRI, the average deformation error inside the region-of-interest (ROI: part of the frontal cortex anterior of corpus callosum towards the sinuses) decreased; and the KLD-based non-rigid registration algorithm utilizing prior information was more effective than the previously developed MI-based global non-rigid registration [5]. An improvement of up to 20% was gained. The KLD-based registration took less than an hour and was 10 to 15 minutes faster than the previous technique for these experiments.

3.2. In-vivo Validation

For in-vivo validation, the developed non-rigid registration technique was applied to 5 MRI datasets obtained from a Siemens Trio 3T scanner. Each dataset included a high resolution T1-weighted anatomical MRI with a spatial resolution of 1.0×1.0×1.1 mm^3, structural T2-weighted turbo-spin echo (TSE) axial scans with spatial resolution of 0.9×0.9×3.0 mm^3, a series of 5 low-resolution fast gradient echo (GRE) EPI with a spatial resolution of 3.5×3.5×3.5 mm^3, a series of 5 high-resolution GRE EPI with a spatial resolution of 1.8×1.8×2.5 mm^3, and a high-resolution dual-echo GRE field map sequence with a spatial resolution of 0.9×0.9×2.5 mm^3. All of the images were initially co-registered to the high-resolution T1-weighted anatomical MRI using the standard affine registration technique of the SPM software package. Non-rigid registration was done between the high-resolution (HR) EPI and each of the two structural MRI scans, i.e. T1- and T2-weighted MRI. The optimized transformation model in each case was then applied to the low-resolution (LR) EPI scans.

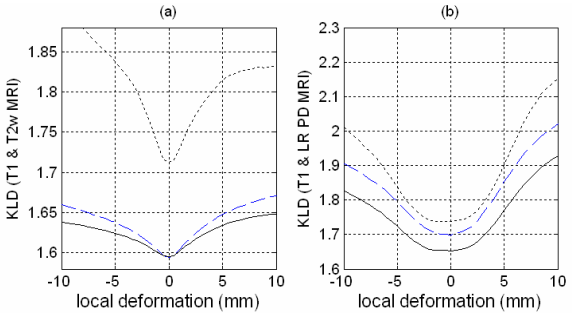

Fig. 1: KLD measure computed between (a) high-resolution T1W and T2W, and (b) T1W and LR PD digital brain phantom images of the *Brainweb* dataset. KLD computed between the reference and test joint *pdf*s on the entire brain by: B-Spline Parzen window estimation (solid), rectangular non-parametric estimation of joint *pdf*s (dashed), and B-Spline Parzen window estimation when the test joint *pdf* is computed on the distortion region only (dotted).

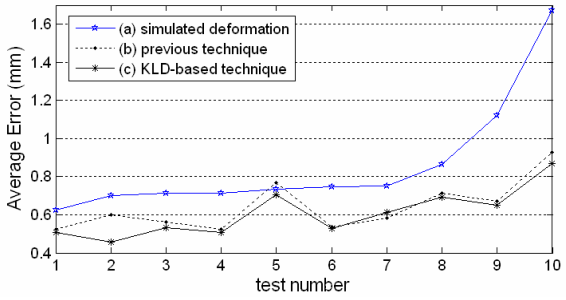

Fig. 2: Average deformation error computed in millimeters in the ROI for (a) ten synthetic deformations on the low-resolution simulated EPI images of the *Brainweb* dataset, (b) after registrations made by the previous MI-based non-rigid registration [5], and (c) after registrations made by the KLD-based technique.

A homogeneous control point spacing of 10×7×10 mm was used on the images. The parameter bound constraints were automatically calculated proportional to the processed phase field map values (a maximum ±9 mm constraint for phase values of ±π rad/sec). A threshold of ±0.1π was used to detect the region of distortion. The deformation field was limited to this region and the reference joint *pdf* was calculated between the images excluding this region. The main parts of the program are developed based on C++ templates and classes of Insight Segmentation and Registration Toolkit (http://www.itk.org). The experiments take

around one hour on a dual processor 3.2 GHz Linux workstation with 4 Gigabytes RAM.

Figure 3 shows that while the registration was done between the HR-EPI and the structural scans, the NMI similarity measure was increased between LR-EPI and both of the structural scans. This can be regarded as an in-vivo validation of the algorithm. The mean and maximum of the deformation field parameters associated with this increase in NMI were 2.58 mm and 7 mm in the distortion region. Finally, Figure 4 shows a sample outcome of the registration algorithm on one of the in-vivo datasets.

4. CONCLUSION

This paper has provided a KLD-based formulation to incorporate field map prior knowledge in non-rigid registration of EPI to structural magnetic resonance brain images. This KLD formulation is based on minimizing the distance between a reference and a test joint *pdf* between the source (EPI) and the target (structural MRI) image. A simplified expression is derived for the derivatives of KLD with respect to the transformation parameters, which makes this formulation computationally efficient as compared to the mutual information formulation. It is shown how phase field map data are used in setting appropriate bound constraints on the transformation parameters. The results obtained through gold standard and in-vivo validation indicate that the developed non-rigid registration technique provides a more effective approach as compared to the previously developed MI-based approach towards registering EPI to structural MRI.

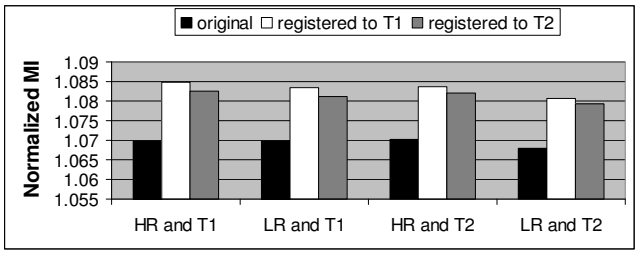

Fig. 3: Normalized MI computed between in-vivo HR and LR EPI and T1- and T2-weighted structural MR images, averaged over 5 real datasets.

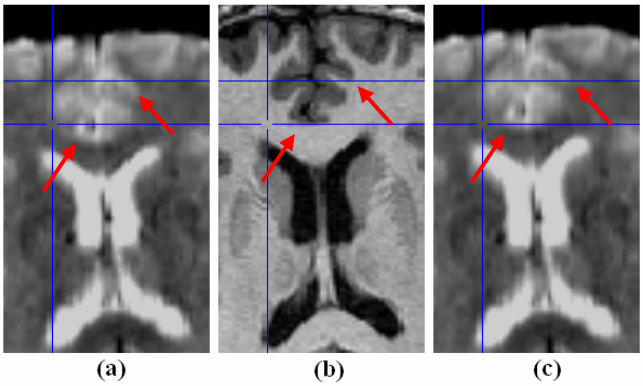

Fig. 4: Sample outcome of the non-rigid registration algorithm; locked cursor axial slices of (a) EPI after affine registration to T1W structural MRI, (b) T1W structural MRI, and (c) EPI after non-rigid registration. The lines and markers point at the visible distortions and their correction.

5. REFERENCES

[1] P. Jezzard, R.S. Balaban, "Correction for geometric distortion in echo planar images from B0 field variations," *Magn. Res. Med.*, vol. 34, pp. 65-73, 1995.

[2] A. Gholipour, N. Kehtarnavaz, R. Briggs, M. Devous, K. Gopinath, "Brain functional localization: A survey of image registration techniques," *IEEE Trans. on Med. Imag.*, vol. 26, no. 4, pp. 427-451, April 2007.

[3] C. Studholme, R.T. Constable, J.S. Duncan, "Accurate alignment of functional EPI data to anatomical MRI using a physics-based distortion model," *IEEE Trans. Med. Imag.,* vol.19, pp. 1115-1127, 2000.

[4] Y. Li, N. Xu, M. Fitzpatrick, V.L. Morgan, D.R. Pickens, B. Dawant, "Physics-based constraints for correction of geometric distortions in gradient echo EP images via nonrigid registration," in *SPIE Proc.: Med. Imag.*, Mar. 2006, vol. 6144, pp. 808-817.

[5] A. Gholipour, N. Kehtarnavaz, K. Gopinath, R. Briggs, M. Devous, and R. Haley, "Distortion correction via non-rigid registration of functional to anatomical magnetic resonance brain images," in *proc. ICIP2006: 13th IEEE Int. Conf. on Imag. Proc.*, Atlanta, GA, Oct. 8-11, 2006, 1181-1184.

[6] R.H. Byrd, P. Lu, J. Nocedal, C. Zhu, "A limited memory algorithm for bound constrained optimization," *SIAM J. Sci. Comput.*, vol. 16, pp. 1190-1208, Sep. 1995.

[7] D. Mattes, D. Haynor, H. Vesselle, T. Lewellen, W. Eubank, "PET-CT image registration in the chest using free-form deformations," *IEEE Trans. Med. Imag.*, vol.22, pp.120-128, 2003.

[8] A. Gholipour, N. Kehtarnavaz, R. Briggs, and K. Gopinath, "A field map guided approach to non-rigid registration of brain EPI to structural MRI," in *SPIE proc.: Med. Imag.*, San Diego, CA, Feb. 17-22, 2007.

[9] T. Cover, J.A. Thomas, *Information Theory*, Wiley, 2006.

[10] A.C. Chung, W. Wells III, A. Norbash, W. Grimson, "Multi-modal image registration by minimizing Kullback-Leibler distance," *Lect. Notes Comput. Sci.*, vol. 2489, pp. 525–532, 2002.

[11] S. Soman, A.C. Chung, W. Grimson, and W. Wells III, "Rigid registration of echoplanar and conventional magnetic resonance images by minimizing the Kullback-Leibler distance," *Lect. Notes in Comput. Sci.*, vol. 2717, pp. 181–190, 2003.

[12] R. Gan, J. Wu, A.C. Chung, S. Yu, W. Wells III, "Multi-resolution image registration based on Kullback-Leibler distance," *Lect. Notes in Comput. Sci.*, vol.3216, pp.599-606, 2004.

[13] C. Guetter, C. Xu, F. Sauer, J. Hornegger, "Learning based non-rigid multi-modal image registration using Kullback-Leibler divergence," *Lect. Not. Comput. Sci.*, vol.3750, pp.255–262, 2005.

[14] P. Thevenaz and M. Unser, "Optimization of mutual information for multiresolution image registration," *IEEE Trans. Imag. Proc.*, vol. 9, pp. 2083–2099, Dec. 2000.

[15] M. Unser, "Splines: a perfect fit for signal and image processing," *IEEE Signal Proc. Mag.*, vol. 16, pp. 22-38, 1999.

[16] D.L. Collins, et al., "Design and construction of a realistic digital brain phantom," *IEEE Trans. Med. Imag.*, vol.17, pp.463-468, 1998.

ACKNOWLEDGEMENTS

This study was supported jointly by the UTD Erik Jonsson School and a subcontract from the Epidemiology Division, Department of Internal Medicine, Univ. of Texas Southwestern Medical Center at Dallas under grant no. DAMD17-01-1-0741 from the U.S. Army Medical Research and Materiel Command. The content of this paper does not necessarily reflect the position or the policy of the U.S. government, and no official endorsement should be inferred.